

## CHAPTER 4

The modelling of short waves in shallow waters.  
Comparison of numerical models based  
on Boussinesq and Serre equations.

M. Brocchini<sup>†</sup>, M. Drago<sup>†</sup> and L. Iovenitti<sup>†</sup>

### Abstract

Two different flow models of the surf zone wave-current dynamics based on Boussinesq and Serre equations have been implemented and tested. Good results were obtained while testing the models against many different wave and current data sets. A preliminary calibration was tried but further activities are required to define the proper parameters.

### Introduction

The research in coastal hydrodynamics recently focused its attention on the mathematical and numerical modelling of the water flows in that region where wave breaking takes place.

This was to fill the gap that shallow water wave theories suffered up to now: they could no longer predict wave-currents characteristics while approaching the surf zone. This was a very serious limit to the application of predictive models to coastal engineering and to environmental problems.

The latest trend in the modelling of such phenomena is to develop flow models that work at space-time scales much smaller than the wave length and period. Those models are based on the solution of the equations derived from the continuity and approximated Navier-Stokes equations. Of particular interest are the Boussinesq equations, the Su-Gardner equations and a particular approximation called the Serre equations. The presence of turbulence and energy dissipation in the breaking region is introduced by the concept of the 'surface roller'.

---

<sup>†</sup> Snamprogetti S.p.A. - Offshore Division

The roller is the upper turbulent region of the wave. The main hypothesis is that the water mass of the roller does not take part in the wave motion, but only contributes to the internal pressure field. Its main action is, then, to extract energy from the wave motion acting on it, as a first approximation, through an hydrostatic pressure contribution in the momentum equations.

The Boussinesq equations

In the following an irrotational (the velocity is the derivative of a potential  $\phi$ ), inviscid fluid with constant density  $\rho$  is considered. The water depth is  $h$  and the surface waves are characterized by an amplitude  $A$  and a wave number  $k$ . For shallow waters (the depth to wavelength ratio is smaller than one), considering weakly non linear and moderate long waves the Boussinesq approximation is valid:

$$O(\epsilon) = O(\mu^2) < 1,$$

where  $\mu = kh$  and  $\epsilon = A/h$ . In the following the unidimensional equation including terms in the order of  $O(\epsilon)$  and  $O(\mu^2)$  is considered:

$$\eta_t + [(h + \eta)\bar{u}]_x = 0, \tag{1}$$

$$\bar{u}_t + \bar{u}\bar{u}_x + g\eta_x = \frac{h}{2}[(h\bar{u})_{xxt}] - \frac{h^2}{6}(\bar{u}_{xxt}), \tag{2}$$

where

$$\bar{u} = \frac{1}{h + \eta} \int_{-h}^{\eta} \nabla \phi dz \tag{3}$$

is the horizontal depth-averaged velocity and where the subscripts represent partial derivatives. The velocity vertical profile is related to the mean velocity through a parabolic equation depending on the vertical coordinate  $z$ :

$$u(z) = \bar{u} - \frac{h}{2}(h\bar{u})_{xx} + \frac{h^2}{6}\bar{u}_{xxx} - z(h\bar{u})_{xx} - \frac{z^2}{2}\bar{u}_{xxx}. \tag{4}$$

These equations have a dispersive behaviour as the phase velocity depends on the wave number  $k$ :

$$C = (gh)^{1/2} \left( 2 - \frac{k^2 h^2}{3} \right)^{1/2} \tag{5}$$

This depedance has been introduced by the  $O(\mu^2)$  term. It may be noticed that the same term causes the pressure field not to be hydrostatic:

$$P = \rho g (\eta - z) + \frac{\rho}{2} (z^2 + 2zh) \nabla \cdot \bar{u}_t. \tag{6}$$

The Serre equations

Using the same procedure of Su and Gardner (1969), expanding the Navier-Stokes equations up to the order  $O(\epsilon\mu^2)$  and considering a slowly varying water depth (the horizontal derivatives of the water depth are neglected at the higher order) the Serre approximation is obtained for  $O(\epsilon) = 1$ , and  $O(\mu^2) < 1$ :

$$\eta_t + [(h + \eta)\bar{u}]_x = 0, \tag{7}$$

$$\begin{aligned} \bar{u}_t + g\eta_x + \bar{u}\bar{u}_x = & hh_x\bar{u}_{xt} + \frac{h^2}{3}\bar{u}_{xxt} + \\ & + h\eta_x\bar{u}_{xt} + \frac{2}{3}h\eta\bar{u}_{xxt} + \frac{h^2}{3} [\bar{u}\bar{u}_{xx} - (\bar{u}_x)^2]_x. \end{aligned} \tag{8}$$

The presence of higher order approximation makes the solution (solitary or cnoidal solutions for example) to be less peaked with respect to the Boussinesq's one (see fig.1)

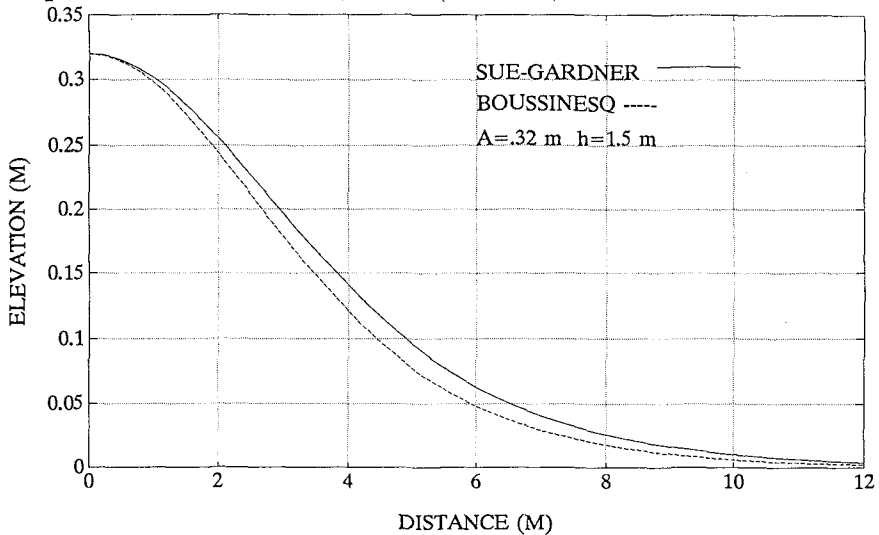


Fig.1 - Solitary solution for Boussinesq and Su-Gardner equations.

The 'Surface Roller'

The description of the breaking process based on the concept of the 'surface roller' was developed by Deigaard (1989). The roller is considered to be that portion of water mixed with air that is formed on the front region of the wave after breaking. The main assumption is that both vertical and horizontal acceleration within the roller are negligible as compared to its other effects on the water beneath. This also means that the pressure field within the roller may be considered hydrostatic. The roller follows the wave crest at a celerity  $C = \sqrt{gh}$ . On these bases the roller may be considered as a solid body that does not take part in the water motion within the wave but only extracts energy from it. This sort of description fits well the spilling breaking process as the overturning of the wave crest and the air-entrainment play a minor role. On the other hand the roller doesn't provide a good representation of a plunging breaker: the overturning of the wave crest generates a too strong jetting within the whole wave to be neglected. Being  $\delta$  the roller elevation above the wave crest and  $\eta$  the wave elevation, the shear stress  $\tau_s$  present at the wave crest-roller interface (Deigaard and Fredsoe (1989)) is:

$$\tau_s dx = -\rho g \delta (\delta_x + \eta_x) dx. \tag{9}$$

It may be deduced that the energy dissipated through a shear stress term in the wave-roller interface is provided by the whole water columns. Considering the spatial derivative  $P_x$  of the Boussinesq pressure vertical profile and neglecting terms in the order of  $O(\epsilon\mu^2)$ :

$$P_x = \epsilon(\eta_x + \delta_x) + \epsilon\mu^2 \left( zh_{xx}\bar{u}_t + 2zh_x\bar{u}_{xt} + \frac{z^2}{2}\bar{u} - xxt \right). \tag{10}$$

This gradient is averaged over the depth giving:

$$\bar{P}_x = \epsilon(\eta_x + \delta_x) + \frac{\epsilon\delta}{h + \epsilon\eta} (\eta_x + \delta_x) - \epsilon\mu^2 \frac{h}{2} (hu)_{xxt} + \epsilon\mu^2 \frac{h^2}{6} \bar{u}_{xxt}. \tag{11}$$

It may be noticed that the Boussinesq equations are obtained neglecting the terms proportional to  $\delta$  and  $\delta_x$ . The dimensional terms due to the roller alone are:

$$\bar{P}_x = -\rho g \left[ \delta_x + \frac{\delta}{h + \eta} (\delta_x + \eta_x) \right]. \tag{12}$$

In the following numerical application this quantity will be multiplied by a factor  $K$  that globally accounts for other energy dissipating phenomena and is calibrated as one of the three 'driving parameters' used in the models. Finally, including the presence of the roller in the mass balance the continuity equation becomes

$$(\eta_x + \delta_x) + [(h + \eta)\bar{u} + \delta C_x]_x = 0, \quad (13)$$

where  $C_x$  is the x-component of the wave celerity.

#### The Roller detection and growth

More consideration is given to correctly represent the surface roller growth from the breaking point toward the shore. Raichlen and Papanicolau (1988) pointed out that the bubble mass on the front face of the wave grows from zero, reaches a maximum and then decreases. Moreover the maximum size of the roller is reached at different distances  $X/h_{br}$  after breaking in dependence on the seabed slope and the breaker type (spilling or plunging). This relative distance ranges between one and ten. In the present model the growth of the roller is governed by the empirical relationship:

$$\delta'(x) = \delta(x) \left[ \frac{\tanh(X/h_{br}) + \tanh(\beta)}{1 + \tanh(\beta)} \right], \quad (14)$$

where  $X$  = distance from the breaking point,  $h_{br}$  = breaking point water depth,  $\beta$  = calibration parameter.

#### The numerical model

Generally speaking, along the curve  $C$  bounding a certain domain  $D$  both open and closed boundary conditions may be encountered. The latter covers all those situations ranging from total reflection to complete absorption. At the open boundaries radiation conditions are applied. They are schematized according to the following relationship:

$$f_{n1} - C\eta = -2C\eta_I f(\alpha), \quad (15)$$

$$u(h + \eta) = f_{n1}, \quad (16)$$

where

$$\begin{aligned} f_{n1} &= \text{outgoing normal flux} \\ \eta &= \text{actual sea surface elevation} \\ \eta_I &= \text{elevation of the incident wave} \end{aligned}$$

$C =$  wave celerity  
 $\alpha =$  the angle between the incident  
 wave and the boundaries

The wave celerity  $C$  is calculated by the appropriate theory: second order cnoidal wave theory. On the other hand the linear theory for shallow waters is applied to determine the celerity for irregular waves. The function  $f(\alpha)$  was firstly evaluated as  $f(\alpha) = 1 + \sin \alpha$ . A numerical analysis carried out with unidimensional and bidimensional models showed that the validity of the above relationship is limited to angles  $\alpha$  close to  $90^\circ$ . The function  $f(\alpha)$  is now considered a calibration parameter of the model, and is empirically evaluated depending on the value of  $\alpha$ . For closed boundaries two different schematizations are used. Total or partial reflection is schematized by the relationship

$$f_{n2} - C(1 - \gamma)\eta = 0, \quad (17)$$

$$u(h + \eta) = f_{n2},$$

where

$f_{n2} =$  incident normal flux  
 $\gamma =$  reflection coefficient ( $\leq 1$ ; 1 for total reflection).

In this case, too, the wave celerity  $C$  is calculated by the appropriate theory: cnoidal for monochromatic waves and linear for irregular waves. Complete absorption is schematized according to a 'sponge layer' approach (Larsen and Dancy, 1983). The 'sponge layer' is simulated by an extension of the model behind the absorbing boundary. In this extension, after each integration time step, the surface elevations and the fluxes are divided by a dumping factor  $\mu(x)$  which is a function of the distance  $x$  from the boundary:

$$\mu(x) = \exp \left[ \left( 2^{-(x_s - x)/\Delta s} - 2^{-x_s/\Delta s} \right) \ln(a) \right], \quad (18)$$

where  $\Delta s$  is the size of the grid mesh and  $a$  is a constant that depends on the number of the grid lines in the 'sponge layer'. As for the behaviour of the roller at the boundaries, it is assumed that there are no incoming rollers from the open boundaries and that they are completely absorbed at the closed boundaries. The basic equations are numerically integrated by a semi-implicit multistep finite difference technique (Brocchini, Cherubini and Iovenitti, (1991)).

The variables are defined on a space-staggered square or rectangular grid. The integration too is staggered in time as the elevations and fluxes are evaluated at half time steps  $(2n + 1)\Delta t/2$ . From the continuity equation (explicit scheme) the water elevation  $\eta$  is calculated, then from the water surface profile a test on the local slope defines the location and thickness of the surface roller. The fluxes are evaluated through the momentum equation (roller contribution included) by a semi-implicit technique made of three different calculation steps.

### Test cases and preliminary calibration

The model has been widely applied to many data sets made available from different European Institutes (Brocchini, Drago and Iovenitti (1992), Drago (1992)). The data sets are relative to wave elevation (Liberatore and Petti (1988), Schaffer (1991), Dette and Oelerich (1991)) and velocity (Quinn et al. (1991)) flume measurements. The waves used in the tests are both monochromatic and irregular; wave breaking occurs over different bottom profiles (sloping or barred). In table 1 a scheme on the analyzed data sets within the validation activities is reported:

Institute	Profile	Type/(Number of tests)	$\frac{H_0}{L_0}$
Padua Un.	Slope 1/30	Irregular (4)	0.0310 ÷ 0.0380
D.H.I.	Barred	Regular (3)	0.0212 ÷ 0.0522
Hannover Un.	Slope 1/20	Irregular (4)	0.0316
Edinburgh Un.	Slope 1/30	Regular (2)	0.0220 ÷ 0.0330

Tab. 1 - Validation data sets.

Table 2 summarizes the percent error  $(H_{exp} - H_{comp})/H_{exp}$  from outside the breaking region to the shore for both Boussinesq and Serre equations.

$\frac{D}{D_b}$	Bouss.	Serre
1.5	+5	+8
1.0	+7	+11
0.6	-15	-8

Tab. 2 - Average percent (%) error on wave height.

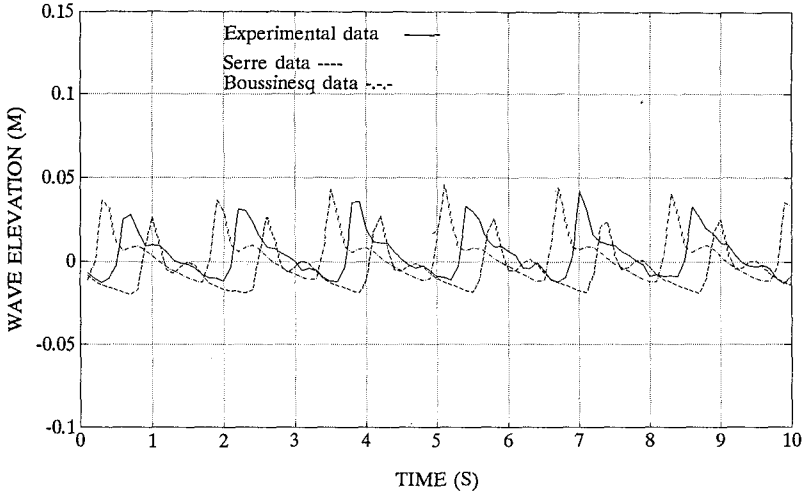


Fig.2 - Wave elevations comparison.  
(Data shifted for better comprehension).

Figure 2 shows an example of computed and measured wave elevation comparison (inside the surf zone) while figures 3 and 4 represent, respectively, a typical comparison of the wave spectra and of the decay pattern for the wave height over a barred profile.

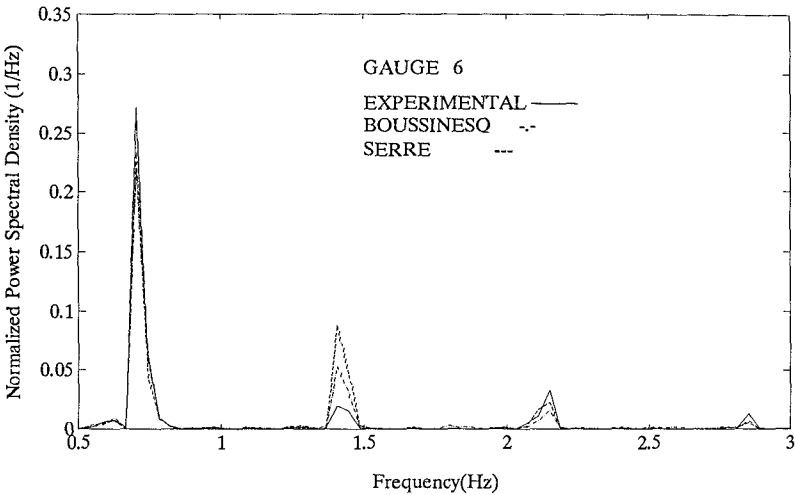


Fig.3 - Wave spectra comparison.

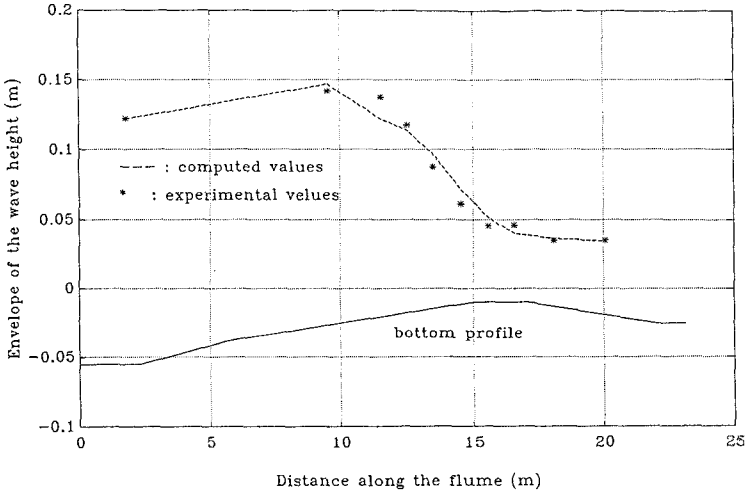


Fig.4 - Wave height decay pattern.

Comparison on velocity data has been worked out both on mean velocity spatial series and on vertical profiles. In fig.5 a typical pattern for mean velocity is shown.

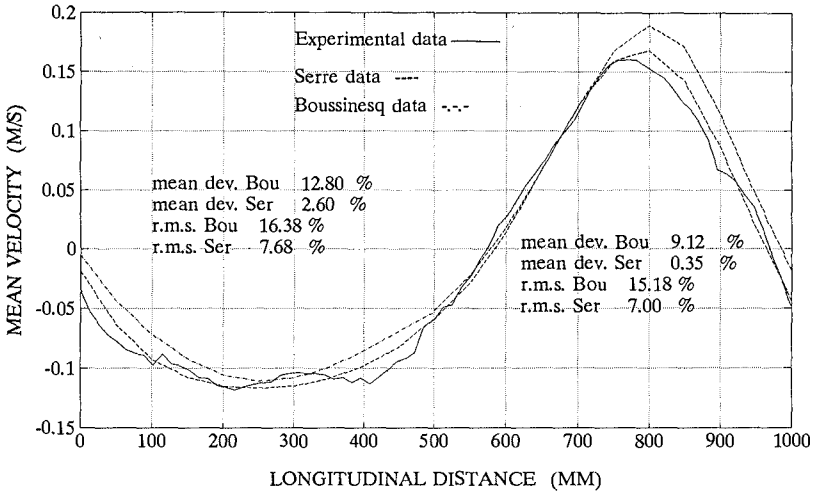


Fig.5 - Mean velocity comparison.

Table 3 sums up the percent error  $(V_{exp} - V_{comp})/V_{exp}$  between experimental and computed velocity profile for two different wave phases and for both Boussinesq and Serre model.

Dist. from bottom(cm)	Crest		Trough	
	Bouss.	Serre	Bouss.	Serre
4.0	-15	-2	-20	-13
6.0	-14	-1	-10	-3
8.0	-9	+3	-5	-5
10.0	-13	-2	+40	+50
12.0	-8	+3		
14.0	-5	+6		

Tab. 3 - Percent error on velocity profiles.

It may be seen that for the maximum phase the Serre model oscillates around the experimental pattern with errors of about 5% while the Boussinesq model gives an almost constant overestimation of the velocity of about 10%. Within the calibration activity typical relationships between wave-seabed characteristics and model breaking parameters ( $\alpha_{br}, K, \beta$ ) were looked for. Thirteen monochromatic wave decay patterns were modelled and compared against the experimental data (Liberatore and Petti (1991)). The experimental waves were characterized by a deep water wave steepness ranging from 0.03 to 0.07 and broke over a submerged bar while eight wave gauges recorded the free water surface from the breaking point to the shoreline. Moreover video camera recordings all along the flume were taken to better evaluate the roller area and the breaking point location.

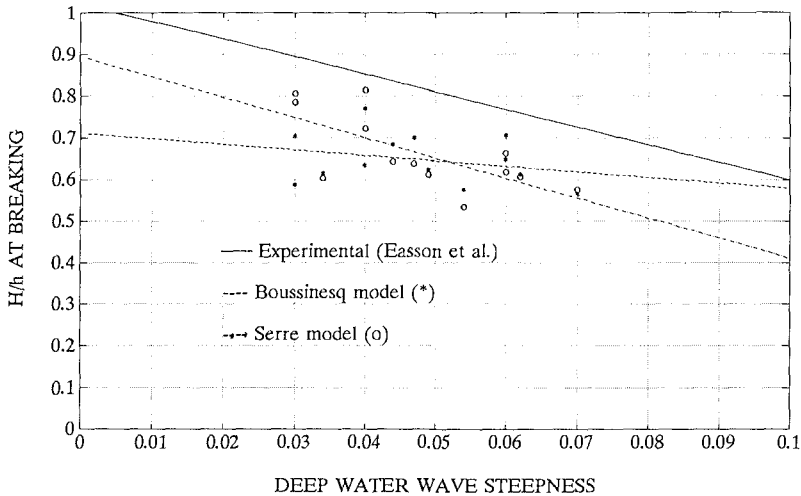


Fig.6 - Adimensional wave height at breaking.

The adopted methodology was to minimize both the differences between the experimental and the computed wave shape and to reproduce the wave height decay pattern all along the flume within a percent error of about 15%. Once the best representation of the wave decay pattern obtained, a first comparison of the results against those coming from wide data sets (Easson et al.(1988)) was tried (see fig.6).

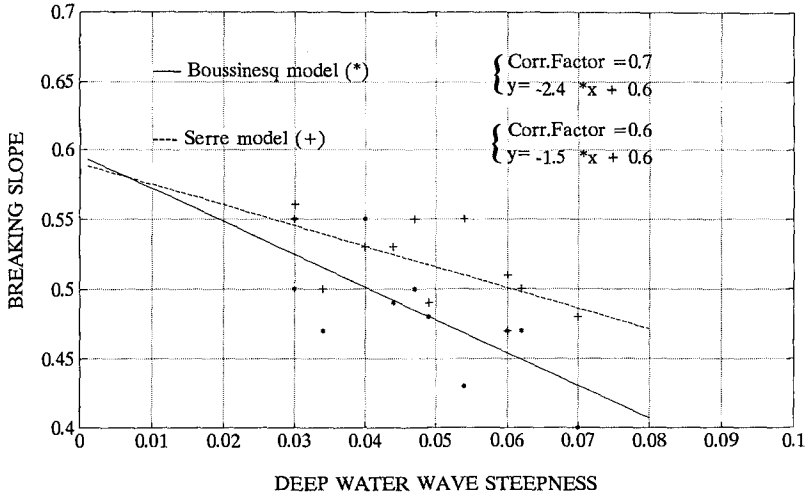


Fig.7 - Preliminary calibration curve for  $\alpha_{br}$ .

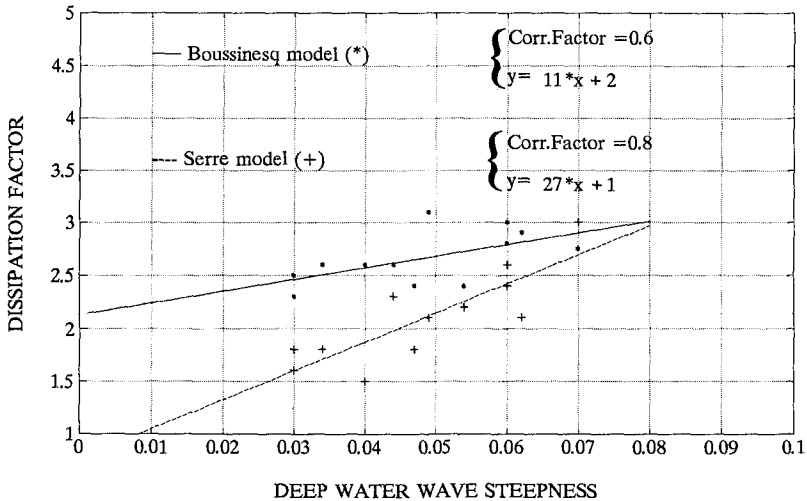


Fig.8 - Preliminary calibration curve for  $K$ .

The underestimation of the  $H/h$  ratio (mainly for the Boussinesq

model) is related to the adopted experimental set-up where the gauges were spaced too far apart to exactly determine the breaking point location. The preliminary calibration curves for the breaking slope  $\alpha_{br}$  and the dissipation factor  $K$  are shown in figures 7 and 8. The correlation factors are not so high as to suggest that the performed calibration is sufficiently reliable. Anyway it is clear that the Boussinesq model needs much higher values for the dissipation parameter with respect to the Serre model to obtain the same energy decay. This is due to the presence of terms proportional to  $O(\epsilon\mu^2)$  which act as a smoothing factor within the surf zone.

### Conclusions

A quite good fit of the experimental wave elevation and spectra has been obtained through the model based on both Boussinesq and Serre equations. A satisfactory description of the wave height decay process in the surf zone was reached (errors of about 15%). The Serre equations give a much better representation of the velocity field than the Boussinesq's. A preliminar calibration of the main parameters was tried but some uncertainties in the determination of the experimental breaking point force a more accurate evaluation on the basis of the camera recordings.

### Acknowledgements

This work was undertaken as part of the MAST-G6 Coastal Morphodynamics Research Programme. It was funded by the Commission of the European Communities, Directorate General for Science, Research and Development, under MAST contract N° 0035-C. The authors wish to thank Mr.Liberatore, Mr.Petti, Mr.Schaffer, Mr.Oelerich, Mr.Dette, Mr.Greated, Mr.Quinn for having provided the data used for models testing and calibration.

### References

- Brocchini, M.,P. Cherubini and L. Iovenitti (1991). An extension of Boussinesq type model to the surf zone. *Proc. 2nd Conf. on Computer Modelling in Ocean Engineering*.
- Brocchini, M.,M. Drago and L. Iovenitti (1992). Modelling of water waves in shallow waters and in the surf zone. *MAST G-6 Final Workshop*, Pisa.
- Deigaard, R., and J. Fredsoe (1989). Shear stress distribution in dissipative water waves. *Coastal Eng.*, Vol.13.
- Deigaard, R., (1989). Mathematical modelling of waves in the surf zone. *Prog. Rep. 69, ISVA, Tech. Univ. Denmark*.

Detle, H. H. and J. Oelerich (1991). Measurements in the Big Wave Flume in Hannover - Individual breaking waves, breaker distribution. *Report N° 1*.

Drago, M. (1992). *Thesis for the degree in mathematical physics - University of Bologna*.

Easson W.J. et al.(1988). Kinematics of breaking waves in coastal regions. *Coastal Eng.*

Larsen, J. and H. Dancy (1983) Open boundaries in short wave simulation: a new approach. *Coastal Engineering*, Vol. 7.

Liberatore, G. and M. Petti (1988) Modifications of random wave characteristics in shoaling waters. *Excerpta*, Vol. 3.

Liberatore, G. and M. Petti (1991) Random wave transformations over a submerged bar. *MAST G-6 Midterm Workshop*, Edinburgh.

Quinn, P.A. et al.(1991) A critical analysis of the particle image velocimetry technique applied to water waves. *Proc. Euro-mech 279 Colloquium*, Delft.

Raichlen, F. and P. Papanicolau (1988) Some characteristics of breaking waves. *Proc. 21st Coastal Eng.*.

Schaffer, H.A.(1991) *Private Communication*.

Su, C.H. and C.S.Gardner (1968) Derivation of the Korteweg-de Vries equations and Burgers equations *Journal of Mathematical Physics*, Vol.10, 3.